11-1-2007

Thermal effects of phase transformations: A review

Alexander Umantsev
Fayetteville State University, aumantsev@uncfsu.edu

ELSEVIER

Thermal effects of phase transformations: A review

A. Umantsev[*]

Department of Natural Sciences, Fayetteville State University, 1200 Murchison Road, Fayetteville, NC 28301, United States

Abstract

All the stages of phase transformations in materials, nucleation, growth, and coarsening, are subject to thermal effects that stem from the redistribution of energy in the system, like release of latent heat, and heat conduction. The thermal effects change the rate and outcome of the transformation and may result in the appearance of unusual states or phases, in particular in nanosystems. This review will cover the attempts of researchers to build a comprehensive theory of thermal effects in different phase transformations. Although the dynamical Ginzburg–Landau (continuum) approach will be used for the analysis of the effects, they are robust and conceivably independent of the theoretical method employed. On general physical grounds a possibility of an oscillatory regime in nucleation is considered and evolution equations for the interfacial motion are derived. The equations show that there are two distinctly different sets of thermal effects of interface motion: one set originates from the existence of the Gibbs–Duhem thermodynamic force on the interface, which has opposite directions compared to the velocity of the interface in the cases of continuous and discontinuous transitions, resulting in a heat trapping effect for the latter and a drag effect for the former. The other set of thermal effects stems from the existence of the surface internal energy and the necessity to carry it over together with the moving interface. As a result, temperature double layers accompany moving domain boundaries after a continuous transition or the surface creation and dissipation effect appear after a discontinuous one. An unusual, novel phase that may appear in isolated nanosystems (adiabatic nanophase) is described. Several experiments are suggested for the verification of the thermal effects in different material systems.
© 2007 Elsevier B.V. All rights reserved.

Keywords: Phase transformation; Dynamics of interfaces; Thermal effects

1. Introduction

Phase transformations in materials occur due to symmetry changes as a result of changing external conditions, temperature, pressure, or chemical potential, and are among the most important factors that influence properties of materials. The 'purpose' of the transformations is to achieve thermodynamic equilibrium in the system under the new external conditions. Depending on the type of symmetry changes in the system, there can be identified two types of transformations: discontinuous (first-order) and continuous (second-order), which differ in dynamics and final outcome. A discontinuous phase transition is manifest by a finite discontinuity in the first derivatives of the appropriate thermodynamic potential, while continuous transitions correspond to singularities in the second derivatives. Continuous transitions are generally characterized by a loss of orientational or translational symmetry elements when different structural variants are possible in a transformed material, for example, domains of different orientation after an order–disorder transition or domains of different magnetization after a ferromagnetic transition.

Phase transformations may be conventionally broken into three stages: nucleation, growth, and coarsening. Nucleation is a general term reserved for the initial stages of phase transformations when a new, incipient phase just emerges in the parent material as a result of thermal fluctuations. On the stage of growth, already coexisting phases separated by interfaces grow at the expense of each other. An interface is an important paradigm in science that helps understand many seemingly unrelated physical situations. Interfaces comprise layers of rapid variations of material's properties and constitute structural defects. Two distinctly different types of interfaces may be identified in the above described transformations: homophase boundaries, which appear after a continuous phase transition and separate two bulk pieces of the same phase with the same composition, e.g. antiphase or magnetic domain boundaries;

---

[*] Tel.: +1 910 672 1449; fax: +1 910 672 1159.
E-mail address: aumantsev@uncfsu.edu.

and heterophase boundaries, which appear as a result of a discontinuous phase transition and separate phases of different crystalline symmetry, e.g., solid/liquid or austenite/martensite boundary. Because of the global disequilibrium of a defective system, a network of interfaces exhibits structural coarsening or time evolution of the interface density. Coarsening is a slow mechanism of establishing global equilibrium with a complete phase separation. On the stage of coarsening the structure of the transformed material changes to fully satisfy requirements of equilibrium thermodynamics.

All stages of phase transformations are subjected to *thermal effects*, which stem from the necessity to redistribute internal energy in the material that undergoes the transformation and may change its dynamical course. Some of the effects are caused by the variation of material properties as a result of temperature gradients that develop during phase transformations, e.g. thermal stress due to thermal expansion or effects associated with the temperature dependence of the coefficient of thermal conductivity. These effects are not considered in the present review, which is devoted to the thermal effects related to the latent heat release and redistribution. The most prominent thermal effects of this nature are dendritic pattern formation during crystallization of pure substances and recalescence during crystallization of alloys. However, these effects are not considered in the present publication because they have been extensively covered in the literature before [1]. Instead, the attention is paid to other, less studied, effects, which change not only the rate but sometimes even the course of a transformation and may result in appearance of unusual equilibrium states or phases; they have come to the attention of the scientific community only lately. One of the purposes of this review is to build a comprehensive theory of various thermal effects on different stages of transformation processes. Many workers have noticed the thermal effects in numerical simulations of non-isothermal transformations and even devised rather sophisticated tools to suppress them [2]. This fact adds to the urgency of a comprehensive theory, which is the subject of the present review. Another purpose of this review is to bring these effects to the attention of experimenters and motivate them on conducting new experiments in the area of phase transitions.

Thermal effects are robust and conceivably independent of the theoretical method employed for analysis, see Section 2. In the present paper we will not be concerned with specific model systems or types of transitions. Rather, we will concentrate on the general picture of phase transformations and try to classify on a comprehensive diagram in the plane of material's parameters different thermal effects, which may manifest in completely unrelated situations. The thermal effects of nucleation are considered in Section 3.1. Numerous thermal effects of interface motion are discussed in Section 3.2. Thermal effects of coarsening are considered in Section 3.3. Equilibrium thermal effects consist in appearance of new equilibrium states or phases and manifest in closed thermodynamic systems where energy is specified and conserved as opposed to an open one. Inhomogeneous in temperature equilibrium states are considered in Section 4.1.

In small (nano)thermodynamic systems the size and energy constrains push the system into another type of a very unusual state, adiabatic nanophase, see Section 4.2. The feasibility of experimental detection of the thermal effects will be discussed in Section 5.

2. Continuum theory of phase transitions

Arguably, the most convenient way of addressing a general problem of transformations in materials is the Landau paradigm of the continuum theory of phase transitions where one assumes that the free energy, in addition to temperature T, pressure and composition, is a continuous function of a set of internal parameters $\{\eta_i\}$ associated with the symmetry changes, which are usually called the long-range order parameters (OP) [3]. The concept of the order parameter helps one to define a phase as a locally stable state of matter homogeneous in the OP's. Different transitions may be laid out into the same framework if proper physical interpretations of OP's are found. We restrict the present paper to the case of a one-component system with a scalar OP, η. Quantitative development of the continuum method originates from a seminal paper by van der Waals [4], where he commenced a systematic study of heterogeneities in thermodynamic systems. Later, Landau [5] considered small heterogeneities in a crystal near the Curie point during X-ray scattering. All cases of phase transformations presented in this paper will be treated here on the common grounds of the dynamical Ginzburg–Landau theory where different transitions correspond to different order parameters in the free energy functional [6]. In the past decade the continuum (field theoretic) method has become very popular in theoretical and computational studies of very different phase transformations in materials: crystallization of pure substances and alloys, precipitation in the solid state, spinodal decomposition, and martensitic transformation [7]. The success of the method is due to its computational flexibility and ability to transcend the constraints of spatial/temporal scales, imposed by strictly microscopic or macroscopic methods, hence becoming a truly multi-scale one with significant predictive power.

2.1. Free energy

Thermodynamic formulation of the theory may be based on a phenomenological expression of entropy of the system as a function of its energy and OP, as it has been done in Ref. [52]. However, we believe that the approach that introduces a phenomenological free energy of the system as a function of its temperature and OP is intuitively more sound and presents more theoretical advantages. As a continuous function of its variables the free energy density $f(T, \eta)$ can be expanded in powers of the OP where only terms compatible with the symmetry of the system are included [3]:

$$f(T, \eta) = f_0(T) + \frac{1}{2}a\eta^2 + \frac{1}{3}b\eta^3 + \frac{1}{4}c\eta^4 + \cdots. \quad (1)$$

The presence of defects (second phase, interfaces) makes the system essentially inhomogeneous even at equilibrium that is, there appear gradients of OP. There is a certain penalty on the inhomogeneous system in the form of the "gradient energy"

contribution and the free energy of the entire system should be taken in the functional form:

$$F = \int \left\{ f(T, \eta) + \frac{1}{2} \kappa (\nabla \eta)^2 \right\} d^3 x. \tag{2}$$

Here the gradient energy is represented in the standard Ginzburg–Landau–Cahn–Hilliard form [5,6,8] and κ is called the gradient energy coefficient. Notice that, in compliance with the Zeroth law of thermodynamics, the expression for the free energy functional cannot include gradients of temperature.

Given the free energy as a function of temperature one can find entropy S and energy E applying the Legendre transformation:

$$S = -\left(\frac{\partial F}{\partial T} \right)_\eta = \int s \, d^3 x; \qquad E = F + TS = \int e \, d^3 x. \tag{3}$$

For equilibrium in an open system it is necessary and sufficient that the variation of its free energy shall either vanish or be positive, $\delta F \geq 0$, for all possible variations of the state of the system, which do not alter its temperature. In the framework of the continuum theory the condition of equilibrium takes the form of the Euler–Lagrange equation:

$$\left(\frac{\delta F}{\delta \eta} \right)_T \equiv \left(\frac{\partial f}{\partial \eta} \right)_T - \kappa \nabla^2 \eta = 0; \quad T = \text{const.} \tag{4}$$

Eq. (4) means that the equilibrium states $\eta^E = \Xi(T)$ are the extremals of the free energy functional, Eq. (2).

The homogeneous part of the equilibrium set $\eta^E = \Xi(T)$ must have at least two minima, η_1 and η_2, corresponding to stable phases, separated by a maximum, which corresponds to an unstable equilibrium state, η_t, called transition state, Fig. 1. A few important parameters may be defined for the system: the equilibrium temperature T_E, the activation barrier height B, and the latent heat L of transformation:

$$f(T_E, \eta_1) = f(T_E, \eta_2);$$
$$B \equiv f(T_E, \eta_t) - f(T_E, \eta_1); \tag{5}$$
$$L \equiv |e(T, \eta_1) - e(T, \eta_2)|.$$

The coefficients a, b, c of the free energy, Eq. (1), reflect important symmetries of the transition and are commonly taken in the Landau approximation where the first one is linearly proportional to the deviation from the critical (spinodal) temperature T_C, $a(T) = a_0 \tau$ with $\tau \equiv (T - T_C)/T_C$, and b, c are temperature independent. The free energy of a system undergoing a *continuous transition* must be an even function of OP because the two equilibrium states are indistinguishable, i.e. two variants of the same phase. This makes the odd-term coefficient b in Eq. (1) vanish. Then, above the critical temperature T_C ($\tau > 0$), the homogeneous part of the equilibrium set $\eta^E = \Xi(T)$ is reduced to only one stable state, viz. disordered phase α with $\eta_\alpha = 0$. Below T_C ($\tau < 0$) this set consists of two stable ordered variants of the same phase, β and γ, with $\eta_\gamma^\beta = \pm\sqrt{-\tau}$ and the unstable disordered (transition) state $\eta_\alpha = 0$, Fig. 2(a). Equilibrium between two ordered variants, β and γ, is possible at any temperature and the latent heat is zero. In *discontinuous transitions* $b \neq 0$ and
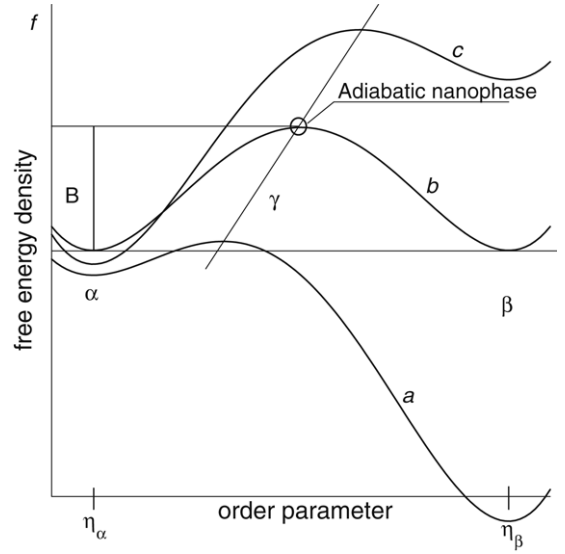
Fig. 1. Free energy density of a system that can undergo a phase transition as a function of an order parameter. Curves a, b, c correspond to different temperatures: (a) $T_C < T < T_E$, (b) $T = T_E$, (c) $T > T_E$. Only a (b)-type curve will be realized for a continuum transition.

the equilibrium set $\eta^E = \Xi(T)$ consists of phases with different symmetries, disordered with $\eta_\alpha = 0$ and ordered with $\eta_\beta(T)$, separated by the transition state $\eta_\gamma(T)$, which is unstable above T_C but gains thermodynamic stability below T_C, Fig. 2(b). The activation barrier B exists at all temperatures above the spinodal one, see Fig. 1, the latent heat L does not vanish, and, in accordance with the Gibbs phase rule, the thermodynamic equilibrium between β and α phases is achieved at the specific temperature T_E only, see Fig. 2(b).

2.2. Interface

Coexistence of two phases at equilibrium entails a transition region between them, called an *interface*, which represents one-dimensional (1D) translation invariant inhomogeneous solutions of the equilibrium set $\eta^E = \Xi(T)$, Eq. (4). As known [9,10], all properties of an interface at equilibrium in a one-component medium may be completely determined by just one intensive quantity, the surface tension or *surface energy* σ which is defined as the excess free energy of the system with an interface, per unit area of the interface, compared to that of the homogeneous bulk ordered or disordered phase occupying the same volume. Then, using Eqs. (2), (4) and the 1D structure of the interface, one can obtain an expression for the surface energy in the continuum representation [8,11]:

$$\sigma = \int_{-\infty}^{+\infty} \kappa \left(\frac{d\eta}{dx} \right)^2 dx. \tag{6}$$

The interfacial thickness determines the characteristic length scale of inhomogeneous solutions and may be defined as follows [8]:

$$l_I \equiv \frac{[\eta]}{\max \left| \frac{d\eta}{dx} \right|}. \tag{7}$$
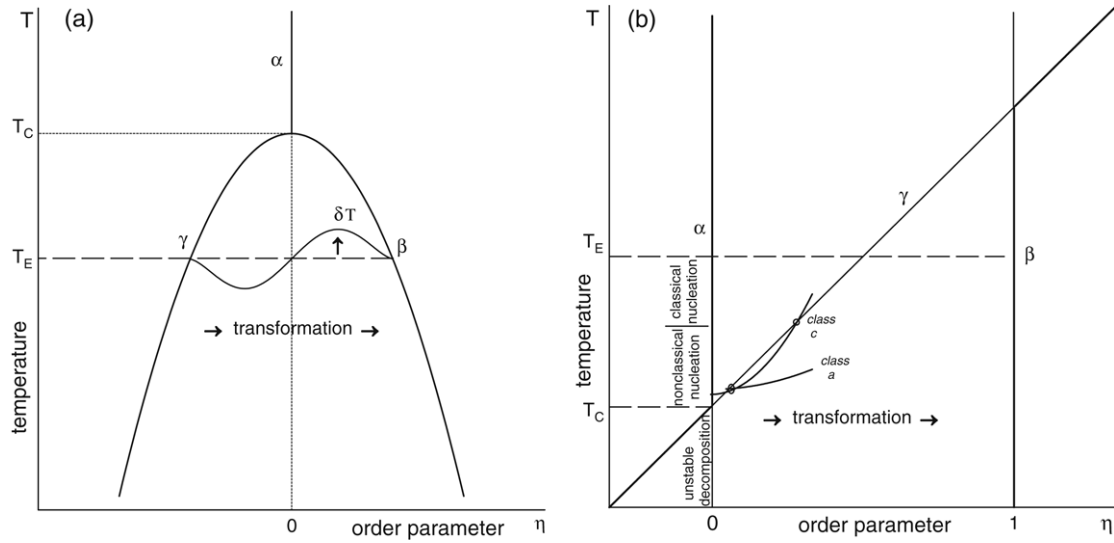
Fig. 2. Homogeneous equilibrium states $\eta^E = \Xi(T)$ for different types of phase transitions. Thick lines—stable states, thin solid lines—unstable states. (a)—continuous transition, curved line—the temperature double layer $\delta T(\eta)$; (b)—discontinuous transition, curved lines—nucleation paths in different systems.

Here and below the quantities in square brackets are defined as $[\varphi] \equiv \varphi_+ - \varphi_- = \varphi(+\infty) - \varphi(-\infty)$ and may be called the jump quantities. Another possibility to define the interfacial thickness is to calculate the distance between the points where the OP reaches the levels of 10% and 90% of its maximum value [57]; usually this definition gives practically the same results as that of Eq. (7).

To elucidate the thermal effects it is advantageous to introduce another measurable (non-diverging) interfacial quantity—the relative surface entropy with respect to the OP [11,12]:

$$\Gamma_s \equiv \int_{-\infty}^{+\infty} \left\{ s - s_+ - (\eta - \eta_+) \frac{[s]}{[\eta]} \right\} dx. \tag{8}$$

One can also introduce the surface entropy χ and surface internal energy ε as follows:

$$\chi \equiv -\frac{d\sigma}{dT}; \qquad \varepsilon \equiv \sigma + T\chi. \tag{9}$$

For continuous transitions $\Gamma_s = \chi$ for all T's. If at equilibrium an interface exists at a specific temperature only, as is the case for a discontinuous transition, differentiation in Eq. (9) may be understood in the sense of disequilibrium because expressions for the surface energy at equilibrium, Eq. (6), and away from it coincide [12]. The equilibrium definition of the interfacial thickness, Eq. (7), may also be extended on non-equilibrium situations of moving boundaries.

In addition to 1D translation invariant solutions, Eq. (4) is known to have many different inhomogeneous isothermal solutions with different symmetries, e.g. cylindrical and spherical [13], one-dimensional periodic [14], and localized pulses. However, none of these possess thermodynamic stability except for 1D translation invariant solutions, which represent two-phase states.

2.3. Dynamics of phase transformations

Away from equilibrium the thermodynamic system relaxes back towards an equilibrium state and an evolution equation for the OP takes the form of the time-dependent Ginzburg–Landau equation (TDGLE):

$$\frac{d\eta}{dt} = -\gamma \left(\frac{\delta F}{\delta \eta} \right)_{T,P} + \zeta(\mathbf{x}, t). \tag{10}$$

A phase transformation is accompanied by energy release and heat redistribution, which give rise to many thermal effects. In order to study these effects, naturally, we need heat equation that accounts for heat releases in the system. Early attempts to describe thermal effects [53] were based on equations which were not consistent with the dynamics of phase transitions, Eq. (10). The issue of thermodynamic consistency for the first time was raised in Ref. [15] and resulted in derivation of the following general heat equation (GHE):

$$C \frac{dT}{dt} = \nabla(\lambda \nabla T) + Q(\mathbf{x}, t) + \xi(\mathbf{x}, t)$$

$$Q(\mathbf{x}, t) = -\left(\frac{\delta E}{\delta \eta} \right)_{V,T} \frac{d\eta}{dt}$$

$$= -\left[\left(\frac{\partial e}{\partial \eta} \right)_{V,T} - \kappa_E \nabla^2 \eta \right] \frac{d\eta}{dt} \tag{11}$$

$$\kappa_E = \kappa - T \frac{d\kappa}{dT}.$$

Later on other groups [52] approached the same problem and derived a similar, but not identical equation. A detailed treatment of this problem and a comparison of different equations were published in Ref. [12].

In Eqs. (10) and (11) C is the specific heat, λ is the thermal conductivity, γ is the response coefficient that sets the time scale of relaxation, $Q(\mathbf{x}, t)$ is the density of instantaneous heat

sources, $\zeta(\mathbf{x}, t)$ and $\xi(\mathbf{x}, t)$ are the sources of Langevin noise with zero mean and δ-correlation functions.

2.4. Universality classes

The free energy, Eqs. (1), (2) and (5), and the system of coupling TDGLE (10) and GHE (11) describes non-isothermal evolution, different regimes of which depend on the thermodynamic, T_E, T_C, C, L, B, κ, and kinetic, λ, γ, properties of materials. Importantly that these eight properties can be arranged into two dimensionless numbers, the thermodynamic number U, and kinetic number R, such that the presence of different thermal effects depends on the magnitudes of these numbers only. This means that all thermodynamic systems may be divided into a few universality classes with similar thermal behavior. Both equations, Eqs. (10) and (11), are of the diffusion type and are characterized by diffusivities, Eq. (11) by the thermal diffusivity $\alpha = \lambda/C$ and Eq. (10) by the ordering diffusivity $m = \gamma\kappa$. The kinetic number R is defined as the ratio of these diffusivities:

$$R \equiv \frac{\alpha}{m} = \frac{\lambda}{C\gamma\kappa}. \tag{12}$$

The thermodynamic number U is the ratio of the relevant energy scales; its definition depends on the type of the transition in question. For instance, for the discontinuous one it is:

$$U \equiv \frac{CT_E B}{L^2}. \tag{13}$$

On the other hand, these numbers may be represented as the ratios of the length scales of the system:

$$U = \frac{l_c}{l_I}; \qquad R = \frac{l_\mu}{l_c}$$
$$l_c = \frac{CT_E\sigma}{L^2}; \qquad l_\mu = \frac{\lambda}{\mu L}; \qquad \mu = \frac{\gamma\kappa L}{T_E\sigma} \tag{14}$$

where l_C is the capillary length, l_μ is the kinetic length, μ is the kinetic coefficient, and we used the fact that $\sigma/l_I \approx B$, which can be recovered from Eqs. (4), (6) and (7). Eq. (14) make it possible to interpret thermal effects as an interplay of different length scales in the system.

3. Different stages of phase transformations

3.1. Nucleation: Emergence of a new phase

When liquid is cooled down below its freezing point the conditions for the emergence of solid phase appear. Depending on the supercooling (supersaturation) of the system emergence of a new phase may take different routes. As it has been pointed out by Gibbs, "In considering the changes which may take place in any mass, we have ... to distinguish between infinitesimal changes in existing phases, and the formation of entirely new phase" [16]. Theoretical methods for the analysis of this process may also differ depending on the magnitude of supercooling. At small supercoolings the new phase appears in the form of small nuclei (droplets) and is characterized by

the nucleation rate that is, the rate of production of droplets larger than the critical size (those that will grow instead of decaying back to the old phase). The classical isothermal theory of nucleation regards a nucleus of a new phase as a small piece of bulk matter surrounded by a geometrical surface with a specified surface energy σ [17]. However, even simple estimates show that the size of the nucleus is comparable with the thickness of its surface. The continuum method avoids this problem and allows a deep and comprehensive inquiry into the problem of nucleation of pure substances and alloys [18]. At large supercoolings the existing phase may reach the point of overall instability, the spinodal point, below which the new phase appears everywhere practically at once in various morphological patterns. The structure of the emerging patterns may be characterized by the two-point correlation function, which plays an important role because its Fourier transform, the structure factor, is directly proportional to the experimentally measurable scattering intensity [19].

Thermal effects of the emergence of a new phase have never been a very popular subject in the literature although several attempts have been made. In their early paper Feder et al. [20] tried to estimate the effect of dissipation of the latent heat on nucleation. They found that for a typical case of 2% water vapor in air the non-isothermal nucleation rate is five times smaller than the isothermal one. However, a systematic study of the effects of the latent heat and finite thermal conductivity on the nucleation rate has not been done yet. Thermal effects in spinodal decomposition of binary alloys have been considered in [21].

When a stable phase is quenched deeply into the vicinity (above or below) of the spinodal temperature in discontinuous transitions (the so-called non-classical nucleation) or undercooled below the critical temperature in continuous transitions, diffuse heterophase fluctuations with small amplitudes far below that of the level of the new phase appear in the system. Their ability to grow depends on the stability properties of the adjacent homogeneous equilibrium states, which may be studied with the help of the linear dynamic stability analysis. In Refs. [22,23] was studied evolution of the small disturbances in the form of harmonic waves, $\{\Delta\eta, \Delta T\} = \{\Sigma, \Theta\} \cdot \exp(\beta t + i\mathbf{k}x)$, superimposed on an equilibrium state in question. Here $\mathbf{k}$ is the wave vector of the permitted perturbations and $\beta(\mathbf{k})$ is the amplification factor, which determines the evolution of the structure factor. When these waves are substituted into Eqs. (10) and (11) as a solution, they yield two simultaneous equations for the amplitudes $\{\Sigma, \Theta\}$, which have a solution only if the following solvability (dispersion) relation is satisfied [23]:

$$\omega^2 + (M-1)\omega + (R+1)\omega q - Rq + Rq^2 = 0 \tag{15a}$$

$$M = \frac{(f_{\eta T}^E)^2}{f_{\eta\eta}^E f_{TT}^E}. \tag{15b}$$

In Eq. (15a) the amplification factor β and the wave number $\mathbf{k}$ were scaled as following: $\beta = -\gamma f_{\eta\eta}^E\omega$, $|\mathbf{k}|^2 = -(f_{\eta\eta}^E/\kappa)q$. In Eq. (15b) the functions f_{ij}^E should be taken at the equilibrium state (not necessarily stable one) and parameter M, called
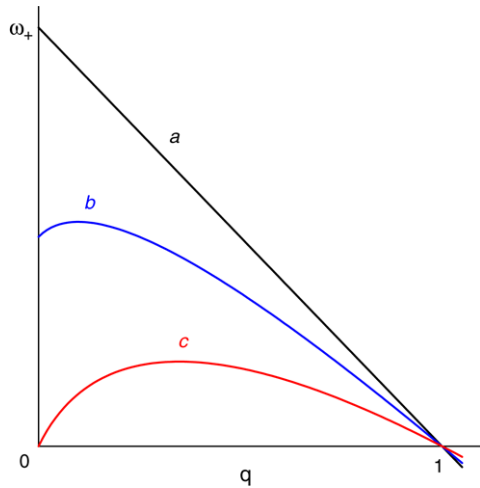
Fig. 3. (Color online) The scaled amplification factor ω_+ for the most unstable branch of the dispersion relation, Eq. (15a), as a function of the scaled wave number q. Parameters: $R = 0.5$; $M = 0.5$ (a); 0.75 (b); 1.5 (c).

the interaction module, determines the strength of interactions between the thermal and ordering modes of the transition. The interaction module of the disordered state α is zero, which excludes any thermal effects around this state. The interaction module of the transition state γ does not vanish and, if estimated at $T = T_E$ ($f_{\eta\eta}^E < 0$), the following is true:

$$M_\gamma(T_E) \approx \frac{1}{7U}. \qquad (16)$$

Thus, as it has been presented in Section 2.4, different regimes of nucleation in discontinuous transformations are determined by the numbers R and U.

The dispersion relation, Eq. (15a), is a second-degree polynomial in two variables whose solutions, as known, are conics with two branches. Analysis of Eq. (15a) shows that both branches are real, at least for the real waves numbers q. Many details of the dynamical nucleation path of the system may be understood from the analysis of the properties of the more unstable branch that is, the one with the greater amplification factor, ω_+, see Fig. 3.

Class a: $0 < M < (R + 1)^{-1}$, *weak interactions.* The uniform mode, $q = 0$, is the fastest one. This is similar to the decomposition in an isothermal system with the only difference that the rate of growth of the modes is determined by the thermal interactions between them, *semi-isothermal nucleation*, see also Fig. 2(b). The mechanism of correlation of initial fluctuations prevails on early stages and creates inhomogeneities on the scale of the cut-off wavelength of instability, $q = 1$. The rate of growth or decay of all waves, however, depends on the coefficient of thermal conductivity, λ. In the limit of $\lambda \to \infty$ one can recover from Eq. (15a) the isothermal form of the dispersion relation: $\beta = -\gamma f_{\eta\eta}^E - m|\mathbf{k}|^2$.

Class b: $(R + 1)^{-1} < M < 1$, *medium interactions.* The uniform wavemode is unstable, but the fastest mode has a finite wave number. Such nucleation regime is more complicated than *Class a* as many different modes are active simultaneously, *hybrid nucleation.*

Class c: $M > 1$, *strong interactions.* The uniform mode is neutral and the wave number of the fastest mode is finite. Thus over this range of conditions the system is unstable with respect to *continuous order parameter modulations*, see also Fig. 2(b).

Case d: $M \gg 1$, *very strong interactions.* From the stand point of thermal effects *Class d* is the most interesting one and deserves a rigorous study beyond the limit of small amplitudes. The nonlinear analysis showed that in this case the growing waves of the new phase obey the nonlinear Cahn–Hilliard equation from spinodal decomposition, so that the order parameter manifests *temporary conservation law* [23]:

$$\frac{\mathrm{d}\eta}{\mathrm{d}t} = \frac{\lambda}{T(f_{\eta T}^E)^2}\nabla^2\left(\frac{\delta F}{\delta\eta}\right)_{T,P}. \qquad (17)$$

The mobility of this regime $\lambda/T(f_{\eta T}^E)^2$ is large and independent of the relaxation constant γ of Eq. (10), which means that such decomposition is totally controlled by heat transfer. The theoretical analysis of this regime motivated two research groups to conduct full-size nonlinear simulations of transformation processes in materials at different levels of instability [22,23]. The simulations revealed a possibility of oscillatory mechanism in a simple one-component system when modulations emerge from the finite wavelength instability of the transition state and create an almost perfect periodic domain structure in the early stages of decomposition [23]. The oscillatory mechanism is analogous to the spinodal decomposition in a system with a conserved OP. The difference is that in the latter case modulations accompany the process from the beginning to end while in the present case the modulations of OP field are temporary and that for a system with a non-conserved OP modulations are governed by energy conservation instead of mass conservation in the spinodal decomposition.

3.2. Growth: Dynamics of interfaces

In this section our goal will be to analyze the dynamics of an interface, which was created as a result of the nucleation process and continues to move under the influence of thermodynamic driving forces that still remain in the system. Consider a transition from one phase to another when the OP changes its value form η_+ to η_-, where $\eta_\pm \in \Xi(T)$. To derive the equation of motion researchers took advantage of the fact that the OP changes very rapidly inside the interfacial transition zone while remaining practically constant or changing very slowly outside this zone, see Fig. 4. Instead of the Cartesian coordinate system $\mathbf{x} = (x, y, z)$, let's introduce new curvilinear time-dependent coordinates $\{u = U(\mathbf{x}, t), v = V(\mathbf{x}, t), w = W(\mathbf{x}, t)\}$ such that OP is a function of one coordinate only: $\eta = \eta(u)$ [24,25,15]. One may introduce the velocity of motion $V_n(v, w, t)$ of the surfaces $U(\mathbf{x}, t) = $ const. These surfaces are equidistant with the radii of curvature $r_u = r_0(v, w, t) + u$, where $r_0(v, w, t)$ and $K = 1/r_0(v, w, t)$ are the radius of curvature and the curvature of the surface $U(\mathbf{x}, t) = 0$, see Fig. 4. Introduction of the time-dependent curvilinear coordinates has an advantage in that the evolution
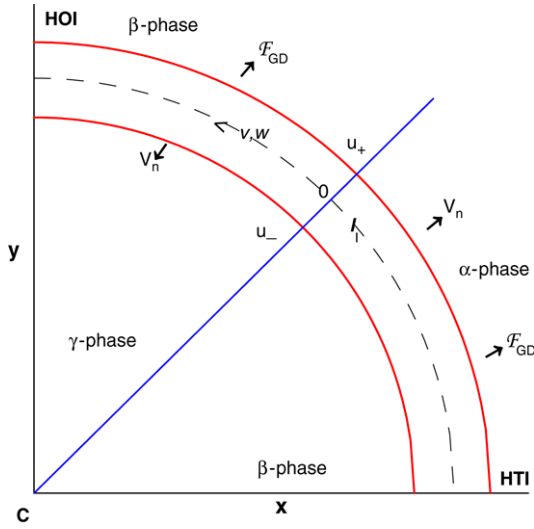
Fig. 4. (Color online) Curvilinear coordinate system (u, v, w) associated with a moving interface. The Gibbs–Duhem force $\mathcal{F}_{GD}$ may be either parallel or antiparallel to the interfacial velocity V_n depending on the type of interface heterogeneous (HTI) or homogeneous (HOI).

of the OP field may be described now by the motion of one surface $U(\mathbf{x}, t) = 0$ in space and time.

If the geometric number of the interface is small enough:

$$Ge \equiv 2|K|l_I \ll 1 \tag{18}$$

the free energy change may be separated into volumetric and interfacial contributions. If in addition to the condition, Eq. (18), the generalized Peclet number is small:

$$Pe \equiv l_I|V_n|C/\lambda \ll 1 \tag{19}$$

then the temperature distribution is a function of the same coordinate u also: $T = T(u)$, the quasi-stationary case. In this case the curvilinear coordinates transform TDGLE (10) and GHE (11) into ODE's as follows [12]:

$$\kappa \left(\frac{d^2\eta}{du^2} + k_\eta \frac{d\eta}{du}\right) - \frac{\partial f(T, \eta)}{\partial \eta} = 0; \qquad k_\eta = 2K + \frac{V_n}{m} \tag{20}$$

$$\lambda \left(\frac{d^2T}{du^2} + k_T \frac{dT}{du}\right)$$
$$+ V_n \left\{\left(\frac{\partial e}{\partial \eta}\right)_T - \kappa_E \left(\frac{d^2\eta}{du^2} + 2K \frac{d\eta}{du}\right)\right\} \frac{d\eta}{du} = 0; \tag{21}$$
$$k_T = 2K + \frac{V_n}{\alpha}$$

where k_η may be called the dynamical curvature and k_T—the thermal curvature of the interface.

In order to derive the evolution equation for a piece of interface we average Eq. (20) over the thickness of the interface that is, we multiply all the terms of this equation by $d\eta/du$ and integrate them over the interval (u_-, u_+), see Fig. 4. Taking into account that $d\eta/du$ vanishes at u_- and u_+ and utilizing the relation $df = (\partial f/\partial \eta)d\eta + (\partial f/\partial T)dT$ we obtain an equation for the motion of a piece of a phase separating interface:

$$V_n \frac{\sigma}{m} = -2\sigma K + [f] + s_+[T] + \mathfrak{I}_{GD} \tag{22a}$$

$$\mathfrak{I}_{GD} \equiv \int_{u_-}^{u_+} (s - s_+) \frac{\partial T}{\partial u} du. \tag{22b}$$

Eq. (22a) reveals the driving forces on the interface; they have the units of pressure because they act on a unit area of the interface. A piece of interface is driven not only by the free energy difference on both sides of the interface, $([f] + s_+[T])$ and the Laplacian pressure $(-2\sigma K)$, but also by another force, $\mathcal{F}_{GD}$, Eq. (22b), which vanishes if the temperature in the transition zone is uniform or the thickness of the latter is zero. This force was called Gibbs–Duhem force [12,26].

To elucidate the physical meaning of $\mathcal{F}_{GD}$ we solve the quasi-stationary GHE (21) for the temperature gradient inside the interface using a method of asymptotic expansion. First, we obtain integral representations of the temperature gradient when the temperature gradient in the final phase at $u = u_-$ is zero. Then we expand it in increasing powers of the thermal curvature of the interface k_T by integrating this expression by parts and retain the terms of the order not higher than $(l_I k_T)$. Such an expansion is possible due to conditions, Eqs. (18) and (19), and may be considered an expansion into "powers of disequilibrium". Then the temperature gradient and the entropy difference in Eq. (22b) can be calculated using the equilibrium structure of the OP, Eq. (4) (for details see Ref. [12]). This gives us the expression for the Gibbs–Duhem force:

$$\mathfrak{I}_{GD} = -\frac{V_n}{\lambda}\left(J_1 - \frac{V_n}{\lambda}CJ_2 - 2KJ_3\right). \tag{23}$$

The coefficients J_i's represent different moments of the entropy density; their exact expressions and values for different types of interfaces may be found in Ref. [12]. It is instructive, however, to elucidate the physical nature of the terms in Eq. (23) using only measurable quantities such as the latent heat L and the relative surface entropy Γ_s, Eq. (8). Taking into account that $[s]_{TE} = L/T_E$ one can find that:

$$J_3 \approx J_2 \approx J_1 l_I; \qquad J_1 \approx \frac{T_E}{l_I}\Gamma_s^2 - \frac{l_I}{6T_E}L^2. \tag{24}$$

The type of transition affects the relative magnitudes of Γ_s and L, which in turn changes the magnitude of J_1 in Eq. (24): J_1 is negative for a typical discontinuous transition and positive for a continuous transition. This means, see Eq. (22a), that $\mathcal{F}_{GD}$ serves as a driving force in discontinuous transitions (propels the motion of a heterophase interface) and as a drag force in continuous transitions (opposes motion of a homophase interface).

Chain substituting Eq. (24) into Eq. (23) and then into Eq. (22a) and taking into account that $[f] + s_+[T] = L(T_E - T_-)/T_E$, we arrive at the evolution equation of interface motion:

$$L\frac{T_E - T_-}{T_E} = 2\sigma K + V_n\frac{\sigma}{m}$$
$$- V_n\frac{l_I}{\lambda}\left(\frac{L^2}{6T_E} - \frac{T_E\Gamma_s^2}{l_I^2}\right)\left(1 - V_n\frac{Cl_I}{\lambda} - 2Kl_I\right). \tag{25}$$

The term in the left-hand side expresses the 'thermal' driving force on the interface, the first term in the right-

hand side expresses the Laplacian pressure on the interface (the Gibbs–Thompson effect), and the last term express the correction due to Gibbs–Duhem force.

Any heat released at the interface should be removed away from it by means of thermal conduction mechanism. To obtain the heat balance equation for a quasi-stationary curved interface we average Eq. (21) in the interval (u_-, u_+) [12]:

$$\lambda \left\{ \left[\frac{dT}{du} \right] + k_T[T] \right\} + (L - 2\varepsilon K) V_n = 0. \tag{26}$$

Eq. (26) differs from the regular heat balance (Stefan) equation in the terms $-2\varepsilon K V_n$ and $k_T[T]$. The first one vanishes for a flat or immobile piece of interface, i.e. when the interfacial area does not vary.

Eqs. (25) and (26) identify the local interfacial variables V_n, K, T_-, $[T]$, $[dT/du]$, and relate them to the thermodynamic interfacial quantities, L, σ, ε, Γ_s, l_I and kinetic properties of the medium like α, m. The beauty of these equations is that they are expressed only through measurable quantities and appropriate thermodynamic parameters of a system and still are applicable to many different situations. These equations are independent of the history of the process and may be used as boundary conditions in a global problem of structural evolution like that of dendritic growth in crystallization or domain growth after continuous ordering. Eqs. (25) and (26) reveal two distinctly different sets of thermal effects of interface motion which will be discussed below. One set originates from the existence of the Gibbs–Duhem thermodynamic force on the interface. Relative to the velocity of the interface, V_n, this force, $\mathcal{F}_{GD}$, has opposite directions in the cases of continuous and discontinuous transitions resulting in the propulsion in the latter and the drag in the former cases. The other set of thermal effects stems from the existence of the surface internal energy and necessity to carry it over together with the moving interface.

3.2.1. Thermal drag

Homophase interfaces (HOI) appear after a continuous transition, when on both sides of the interface are different variants of the same phase; antiphase domain boundaries and magnetic domain walls are examples of HOI's. Motion of HOI has been addressed in numerous studies, which go back to Lifshitz's seminal paper [27] where he conjectured a linear proportionality between the speed and curvature of a moving antiphase domain boundary. Allen and Cahn [25] used a continuum approach, similar to that of the present paper to the motion of an isothermal HOI, and, on the premise of the invariable interfacial profile in the direction of its motion, showed that a small piece of a gently curved interface, condition Eq. (18), will move with the velocity $V_n = -2mK$. Conventional logic dictates that HOI's do not cause temperature gradients and/or thermal effects because the latent heat of the transformation that generates them is zero. What is overlooked by such logic is contribution of the surface internal energy associated with the interface. The influence of the internal energy excess on the dynamics of HOI was considered in [26] in the framework of the Onsager theory of linear response;
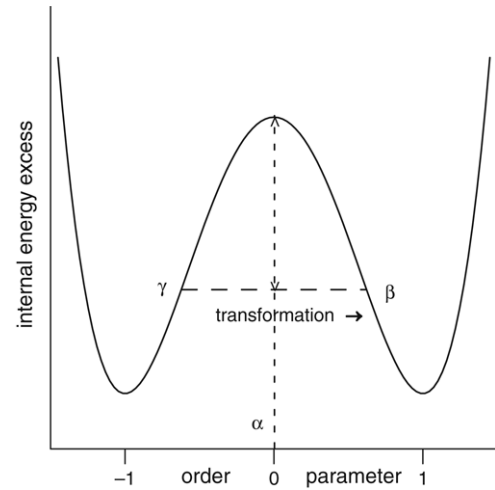
Fig. 5. Borrow–return mechanism. Internal energy of a substance as a function of an order parameter.

the analysis showed that such excess slows down the HOI and causes the *thermal drag effect*:

$$V_n = -\frac{2mK}{1 + D}; \quad D = \frac{m\chi\varepsilon}{\lambda\sigma l_I}. \tag{27}$$

Eq. (27) shows that HOI moves towards the center of its curvature with a speed which is lower than that predicted by the Lifshitz–Allen–Cahn theory [27,25] because the Gibbs–Duhem force is antiparallel to the boundary velocity and plays a role of a drag force, see Fig. 4. The interfacial dynamics is limited not only by the mobility of an interface m but also by the thermal conduction with the drag coefficient D measuring the relative role of these processes. Notice that Eq. (27) can be derived from Eq. (25) if one takes into account that $L = 0$, $\Gamma_s = \chi$ and $\varepsilon \approx T_E\chi$ for this type of transition.

The simplified Onsager-type formulation of Ref. [26], however, did not shed any light on the mechanism of thermal drag. To explain the drag effect we proposed a borrow–return mechanism in the framework of the continuum theory [12]. Both variants on either side of the interface are characterized by the same amount of internal energy density, see Fig. 5. Transformation inside the interface from one variant to the other, however, requires crossing the internal energy barrier (maximum), which corresponds to the disordered phase with $\eta_\alpha = 0$. Then, a small volume of substance must borrow a certain amount of energy from the neighboring volumes while moving 'uphill' on the internal energy diagram, Fig. 5, and return it later on the 'downhill' stage of the transformation. The borrow–return mechanism entails the internal energy flux vector, which requires a transport mechanism, served here by the heat conduction. Thus the drag effect is due to finite rate of heat conduction measured by the conductivity, λ. Thermal drag occurs because the conversion of one variant into another is accompanied by the transmission of energy between neighboring pieces of a material, which cannot occur infinitely fast. Importantly to note again that the thermal drag exists despite of the vanishing latent heat of the transition, which causes thermal effects in discontinuous transformations.
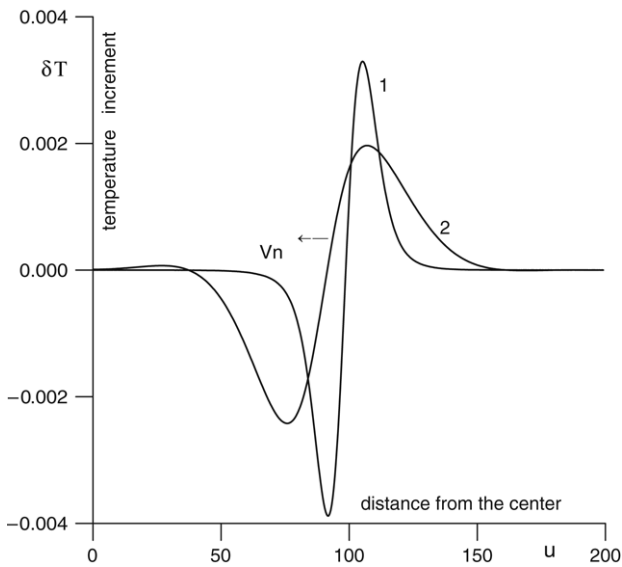
Fig. 6. Temperature waves around homophase interfaces after a continuous phase transition. Curve 1: $\lambda = 0$ (ideal insulator), interface is stationary (ITES). Curve 2: $\lambda > 0$, interface is moving, arrow shows the direction of motion.

3.2.2. Temperature waves

The energy flux through the interface is manifested in the *temperature waves* of amplitude $[T]$, which can be calculated from Eqs. (26), (27) and (12) assuming that $[dT/du] = 0$:

$$[T] = -\frac{2\varepsilon K}{C(R - 1 + RD)} \approx -2T_C \chi \frac{m}{\lambda} K \propto (-\tau)^{1/2} K. \quad (28)$$

Moving HOI creates a temperature wake. The amplitudes of the waves are proportional to the curvature of the interface and critically dependent on the temperature of transformation because $\sigma \propto \sqrt{-\tau^3}$, see also Eq. (9). The simulation results in [12] found such temperature waves in the form of double layers δT of amplitude $[T]$, see Fig. 6. According to (27), motion of HOI slows down in a poorly conducting material. Yet, a more interesting situation happens in an ideal thermal insulator that is, a material with $\lambda = 0$ (see also Section 4.1), where the HOI creates a temperature double layer and stops completely (see Figs. 6 and 2(a)). Although stability of curved HOI's is quite surprising (recall that critical nuclei in the theory of discontinuous transformations are equilibrium but unstable states of the system), it has a simple physical explanation, see Eq. (22a). 'Dissolution' of a small particle of a minority variant is caused by the Laplacian pressure from the curved interface. At the same time, the Gibbs–Duhem force generates the thermal pressure in the particle that opposes the Laplacian pressure. In the ideal insulator these pressures neutralize each other.

3.2.3. Heat trapping

Heterophase interfaces (HTI) separate contiguous phases of different symmetries and appear as a result of discontinuous transitions e.g. solid/liquid or martensite/austenite. Isothermal effects of HTI motion in the framework of a continuum theory have been thoroughly investigated in Ref. [24]. Eqs. (25) and (26) reveal different thermal effects of HTI motion. In the classical theory there are two different regimes of growth of

a low-symmetry β phase at the expense of a supercooled high-symmetry α phase (lines 1 in Fig. 7): the diffusion-controlled regime when the growth velocity V_n decays in time [54] and the kinetics-controlled regime when V_n has the stationary value [55]. The former takes place when the initial temperature of the α phase is $T_0 > T_E - L/C$, the latter—when $T_0 < T_E - L/C$ [56]. But the temperature of the β phase, T_-, never exceeds the equilibrium temperature: $T_- \to T_E$ in the diffusion-controlled regime and $T_- = T_0 + L/C < T_E$ in the kinetics-controlled regime. The latter relation may be obtained from Eq. (26) applied to a plane interface if the jumps are calculated between the far-field quantities: in this case $[dT/du] = 0$ and $[T] = T_0 - T_-$. The continuum theory (Eq. (25) and lines 2 in Fig. 7) reveals a possibility to have the β phase growing ($V_n > 0$) from the supercooled α phase even when the temperature of the β phase after transformation is above the equilibrium value ($T_- > T_E$), e.g. growth of superheated ice from supercooled water. This effect was called *heat trapping* in [28] by analogy with solute trapping. The heat trapping may happen in a narrow interval of initial temperatures $T_E - L/C < T_0 < T_{tr}$ where the stationary regime of growth sets in instead of the decaying one. Eq. (25) can be used to find the condition for the heat trapping to be possible: the coefficient of the linear in V_n term must be negative. Taking into account that Γ_s for discontinuous transitions is small the following criterion must be fulfilled:

$$RU = \frac{\lambda}{\mu L l_I} < \frac{1}{6}. \quad (29)$$

Criterion (29) may be considered as the upper limit on the rate of thermal conduction in the system for the heat trapping to be possible. Given the definitions of the length scales in the system, Eqs. (14), criterion (29) may also be interpreted as that the low limit of the thickness of the interface is six times the kinetic length. Eq. (22a) points out that the heat trapping occurs when the Gibbs–Duhem force becomes large enough to propel an interface against the negative bulk driving force: $([f] + s_+[T]) < 0$. The heat trapping effect was first theoretically predicted in [15]; other workers also noticed this effect in their theoretical calculations [29]. Recently this effect was found to be important for shape memory alloys [30] where it accounts for stick–slip motion of the martensite/austenite boundaries.

Eq. (25) also points at another situation when the growing phase may be observed at a temperature above equilibrium one that is, around regions in materials where the curvature is negative (the center of curvature is in the parent phase). Such situation occurs, for instance, in cavities between the branches of growing dendrites. The difference is that the heat trapping is capable of producing metastable equilibrium phases while dendritic overheating is only a transient. Eq. (25) also implies that the size of the critical nucleus changes in ideal insulators (the systems with $\lambda \to 0$). However, such systems have not been studied in depth yet.
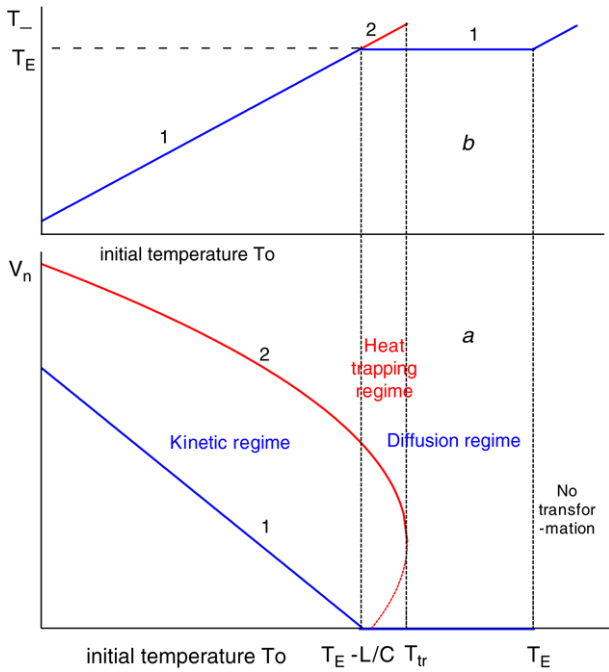
Fig. 7. (Color online) Comparison of the classical and continuum theories of interface motion in a discontinuous transformation. Lines 1 (blue)—the classical theory; lines 2 (red)—the continuum theory. (a)—Interface velocity V_n versus the initial temperature of the α phase; the line 2 is the solution of Eq. (25) for a plane interface ($K = 0$). (b)—Final temperature of the β phase T_- versus the initial temperature of the α phase.

3.2.4. Surface creation and dissipation

Another example of a thermal effect comes from the analysis of the heat balance before and after a HTI sweeps material during a discontinuous transformation. The amount of heat released is called the heat of transformation. It is commonly considered to be equal to the product of the latent heat and the transformed volume. However, as Eq. (26) demonstrates, if the moving interface is curved, the heat of transformation will differ from the above described amount by the amount of the surface area created or destroyed ($\int 2K V_n \mathrm{d}v \mathrm{d}w \mathrm{d}t$) times the surface internal energy ε. This effect, which may be called the *surface creation and dissipation effect*, has been noticed by Wollkind [31] and used in the form of a boundary condition in one of his later papers. Tiller discussed the surface creation or destruction effect in his book [32]. However, the theoretical description of this effect in Ref. [32] was not accurate because the author attributed it to the evolution equation, similar to Eq. (25), instead of the heat balance condition, Eq. (26). The rigorous derivation of the surface creation and dissipation effect has been given in Ref. [15] and used in Ref. [33] to study the influence of this effect on the absolute stability of the solidification front during crystal growth from a hypercooled melt, i.e. the condition when the front looses dendritic or cellular structure and restores completely the morphological stability. The surface creation and dissipation effect destabilizes the crystallization front because it reduces the amount of heat released by a growing bump, hence reduces its temperature T_- and increases its velocity V_n, see Eq. (25).

3.3. Coarsening: Approach to equilibrium

It is customary to view coarsening as a curvature-driven motion. In this case, there would be no coarsening in 1D systems where all boundaries are flat. In fact, coarsening is driven by the reduction of surface energy, which makes coarsening subjected to thermal effects. Analysis of coarsening scenarios in several closed systems revealed the mechanism of *the sequential doubling of the structural period* (spacing), which is completely different from the traditional Lifshitz–Slezov–Wagner mechanism of coarsening. In Ref. [23] a discontinuous phase transformation in a 1D system was analyzed under conditions of thermal isolation. The coarsening process was found to start practically immediately after the emergence of the almost perfect periodic domain structure and take one of two types of routes: dissolution of a layer accompanied by a local temperature dip or coalescence of two neighboring layers accompanied by a temperature spike. Both types eventually lead to a new equilibrium state with the double period. The 1D system under study was not the only example of period doubling effect during coarsening after discontinuous transformation. Numerical simulations of dendritic growth showed that the coarsening process of the sidebranch structure during growth stage also exhibits mechanism of period doubling [34,35], which was substantiated by direct experimental observations of growing dendrites of succinonitrile [36] and ammonium bromide [37]. When the volume fraction of coarsening domains is rather high the coarsening process is a result of strong long-range interaction between them through the temperature field. Thus the mechanism of sequential period doubling is robust for coarsening in 1D or quasi-1D (dendritic branches) systems with a conserved quantity.

4. Equilibrium in closed systems

Equilibrium thermal effects appear in closed systems, where exchange of energy with the ambience is prohibited. The problem of equilibrium in closed systems is described by maximization of the entropy functional for constant energy functional, see Eq. (3). In mathematical terms, it is formulated as an isoperimetric problem from the calculus of variations. Analysis of isolated systems [28,38,39] revealed that almost all equilibrium states obey the same uniform-temperature conditions as in open (isothermal) one, see Eq. (4). However, unlike in the open system where the global thermodynamic equilibrium is reached at a completely homogeneous state, in closed systems thermodynamic equilibrium may have a structure that is, may be a heterogeneous mixture of coexisting phases of the same temperature, if the total energy of the system belongs to a certain band [38,39].

4.1. Inhomogeneous in temperature equilibrium states

In addition to common, uniform-temperature equilibrium states, there exist unique, closed-system equilibrium states, which are not possible in open ones. These equilibrium states
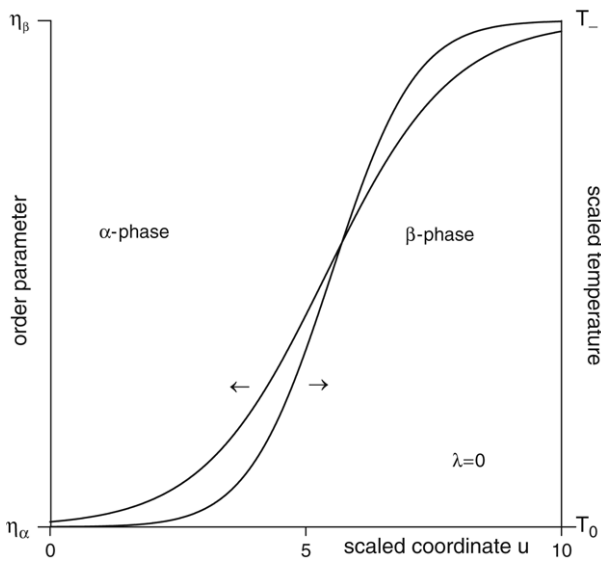
Fig. 8. Distributions of temperature (scaled with L/C) and order parameter as functions of the coordinate u (scaled with l_I) for an inhomogeneous in temperature equilibrium state (ITES) after a discontinuous transition.

are represented by extremals of the functionals of entropy S and energy E simultaneously, Eq. (3). Such states are characterized by a non-uniform temperature distribution and were called *inhomogeneous in temperature equilibrium state* (ITES) [28]. For the case of a discontinuous transition ITES represents a two-phase state of coexistence of the terminal phases, α and β, the same phases as in the isothermal state. However, the temperature of the state changes together with the order parameter (see Fig. 8). Analysis of the thermodynamic stability of ITES showed that this state is not absolutely stable but of the saddle-type stability. Nevertheless such states are important because the system may spend a great deal of time in the vicinity of the state during a transformation process. ITES can be achieved in a thermodynamic system with the vanishing thermal conductivity that is, ideal thermal insulator. Another example of ITES is the temperature double layer, which may appear after continuous transformation (see Section 3.2.2 and Fig. 6). The variational nature of the latter state, unfortunately, is not known to the author.

4.2. Adiabatic nanophase

Reduction of the size of a thermodynamic system undergoing a discontinuous transition brings up another interesting and unusual equilibrium thermal effect. This effect consists in the stabilization of the transition state γ in very small particles of some materials. The most striking feature of this result is that the transition state possesses *maximum free energy* among all other homogeneous states of the system at the same temperature, see Fig. 1. Stabilization of the transition state is a completely equilibrium effect, which comes about as a result of two mutually assisting constraints: insulation and confinement. That is why such state was called the *adiabatic nanophase* (ANP) [39]. A thermodynamic stability analysis carried out in [39] revealed that for the ANP to be possible certain criteria should be met. On the one hand, the material's properties should

be restricted to certain values: the thermodynamic number U must be less than the critical value $U_{\text{cr}} \approx 3/32$. On the other hand, there exists the critical thickness

$$X_{\text{cr}} \equiv \frac{\sigma}{B} \tag{30}$$

such that in layers of thickness less than the critical $X < X_{\text{cr}}$ creation of a phase separating interface is not favorable and the transition state turns into the global optimizer—ANP. Linear dynamic stability analysis, Eq. (15a), confirms the inference of the thermodynamic stability of ANP in layers of thickness $X < X_{\text{cr}}$. This makes the transition state globally stable not only with respect to the bulk phases but with respect to the heterostates also.

5. Experimental verification

In this section we will discuss the possibilities of experimental verification of the theoretical findings presented in this review. The problem of practical application of different thermal effects is more complicated and for the most part will be left out of the present discussion. As one can see from Eqs. (25)–(28), dynamical thermal effects are inversely proportional to the coefficient of thermal conductivity, which greatly reduces chances of finding such effects in metallic systems where the thermal conductivity is rather high. However, we expect these effects to be significant for phase transitions in organic and colloidal systems, which are becoming a very popular subject of study now.

5.1. Continuous transitions

In Section 3.2.1 we showed that the heat conduction in a material that had undergone a continuous transition causes thermal drag, which is important for the motion of HOI's that appear after the transition. This should be taken into account in experimental verification of the theory of coarsening of HOI structure albeit thermal drag does not change time exponents of the latter. According to Eq. (27) the thermal drag effect consists in slowing down the interface and becomes significant when number D is comparable to unity; if $D \gg 1$ the thermal conduction becomes the rate controlling factor. Analysis of the temperature dependence of this number conducted in [26] shows that it can be represented as follows: $D = D_0(-\tau)^{2(\beta+\nu-1)}$ where $D_0 = mk_B/\lambda\Omega$, k_B is the Boltzmann's constant, Ω is the atomic volume; β and $(-\nu)$ are the critical exponents respectively of the order parameter and correlation length near T_C. Hence, the thermal drag is significant if $D_0 > (-\tau)^{2(1-\beta-\nu)}$, see Fig. 9. Depending on the critical exponents β and ν two different situations may be encountered. If $(\beta + \nu) \geq 1$ the thermal drag is significant only when the coefficient $D_0 > 1$; if $(\beta + \nu) < 1$ the thermal drag may be significant even when the coefficient $D_0 < 1$. In the latter case, however, the temperature of the system must be close enough to the critical one $(-\tau) < D_0^{1/2(1-\beta-\nu)}$—critical slowing down. In the case of non-critical slowing down $(\beta + \nu \geq 1)$ the thermal drag manifests in the temperature waves
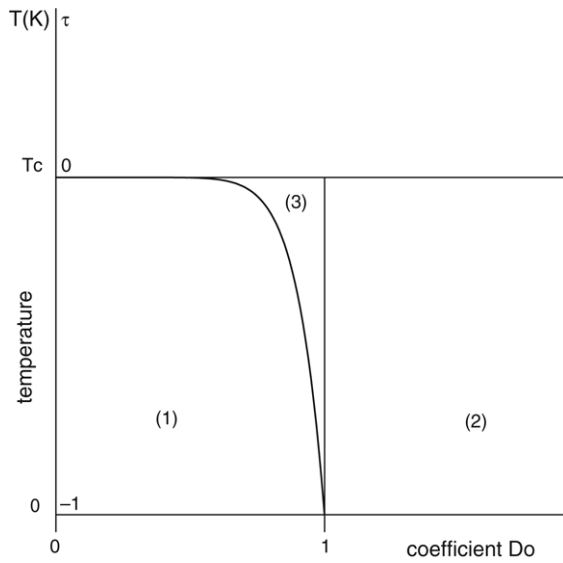
Fig. 9. Diagram of different cases of the thermal drag effect when $(\beta + \nu) < 1$. (1) $D < 1$, the thermal drag effect is not significant; (2) $D > 1$, the thermal drag effect is significant; (3) the critical slowing down: the thermal drag effect is significant even if $D_0 < 1$.

of amplitude described by Eq. (28), which means that small bubbles of vanishing variants should "light up" the brightest before ultimate disappearance. Then Eq. (28) allows us to estimate the maximum temperature wave amplitude $[T]_r$ that may be produced by of a bubble of radius r:

$$[T]_r = \frac{k_B T_C m}{\Omega \lambda r} l_I (-\tau)^{2(\beta + \nu) - 1}. \tag{31}$$

Using very conservative estimates from the available data on metallic systems, the bubbles of 10^{-6} m can produce the waves with amplitudes of 10 °C. In physical experiments the imaging of the temperature waves can be achieved by different experimental techniques. One possibility is *in situ* observation in infrared light. Another possibility is the Mirage technique measurement, which utilizes the gradients in the index of refraction of air arising from the temperature gradients induced by the temperature waves on the specimen surface [40].

5.2. Discontinuous transitions

Existence of different thermal effects in discontinuous transitions depends on the kinetic and thermodynamic numbers and may be summarized in the plane (R, U), Fig. 10. Different regimes of non-classical nucleation, *Classes a, b, c, d* of Section 3.1, find their places in the plane (R, U) due to relation Eq. (16). The modulation mechanism of discontinuous transformation represents an alternative to the classical nucleation and growth for a strongly metastable system. However, even if the parameters of the system fall into *zone (c)* of Fig. 10, achieving the conditions necessary for such mechanism in a specific system will of course depend on the ability to suppress competing nucleation during preceding cooling. Heat trapping regime of interface motion is possible if condition, Eq. (29), is fulfilled, which is realized below the hyperbola on the diagram, Fig. 10. Even in this case the
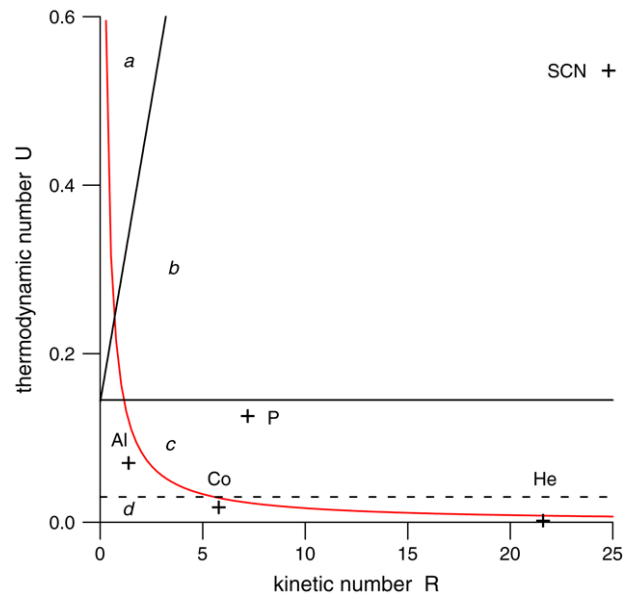
Fig. 10. (Color online) Thermodynamic U and kinetic R properties of different substances and their predicted thermal behavior in crystallization. Zones: (a)—weak interactions, (b)—medium interaction, (c)—strong interaction, (d)—very strong interaction of thermal and ordering modes. ANP is possible in zone (d). Heat trapping is possible below the hyperbola $R = 1/6U$ (red line).

heat trapping effect will be competing with morphological instability of the moving interface.

The thermodynamic condition for ANP, $U < U_{cr} \approx 0.1$ [39] will be fulfilled in zone (*d*) of Fig. 10. Of course, another condition, Eq. (30), must also be fulfilled for this phase to be possible. In small 3-D particles the ANP effect is enhanced by the dimensionality of the system as compared to the 1-D layers considered in Ref. [39]. Before the transition the system should be prepared in the supercooled state and isolated from the environment after that. Notice that, while heat transfer outside the system is not permitted, the thermal conduction inside the system is normal so, that ANP may be found in normal materials, not only ideal thermal insulators. If one opens the system up and exposes ANP to the heat exchange with a thermal reservoir at the same temperature, the delicate balance of such phase will be destroyed and the equilibrium will be shifted in the direction of β or α phase. The properties of ANP allow one to use such materials as sensors of insulation. Analysis of the diagram in Fig. 10 reveals that from the vantage point of thermal effects most interesting are materials with small values of U and R.

The numbers U, R can be estimated only for a handful of real materials and transformations because the interfacial and kinetic properties are hard to find in the literature: number R can be estimated if the kinetic coefficient μ is known, number U needs the knowledge of σ and l_I independently. Kinetic coefficients, for instance, may be extracted form the comparison of experimental and theoretical results on dendritic growth [41, 43–46]. The interfacial thickness is the most difficult parameter to measure even for the most studied transformation that is, crystallization. Recognition by many researchers that these parameters are of great importance led to the development of novel first-principles and molecular dynamics methods that

Table 1
The melting temperature $T_E(K)$ and thermodynamic U and kinetic R numbers for different elements and substances in crystallization

Quantity Substance	T_E (K)	$U \times 10^2$	R	References
Aluminum	939.30	7.03	1.38	[47]
Cobalt	1765.15	1.77	5.78	[41]
Copper	1356.15	4.55	59.0	[41]
Helium	35.04	0.186	21.6	[45]
Nickel	1725.15	14.5	40.4	[41,42]
Lead	600.65	7.70	501	[46]
Phosphorus	317.10	12.6	7.19	[43]
Silver	1234.15	6.37	113	[41]
Succinonitrile	331.24	53.6	24.8	[44]

allow to estimate these parameters numerically [47,57]. In Table 1 one can find numbers U and R for crystallization of some elements and substances. The solid/liquid interfacial thickness was estimated here as 1 nm for all materials. The substances, which are the best candidates for thermal effects are also labeled on Fig. 10. Juxtaposition of the real material properties with the theoretical calculations in Fig. 10 shows that the most interesting effects such as continuous modulations, heat tapping, or adiabatic nanophase are possible for crystallization of some of these substances.

Actually, it is quite possible that examples of ANP have already been seen in different experimental systems without clear recognition of this fact. Kajiwara, Ohno, and Honma [48] studied martensitic transformation in nanoparticles of pure Co and Co–Fe alloys. They found that, instead of a stable bulk phase (4H), a previously unknown phase (2H) forms in the nanoparticles when they are rapidly cooled in vacuum. To interpret these experimental results Suzuki and Takahashi [49] numerically studied the nucleation mechanism in adiabatic martensitic transformations in crystals composed of particles interacting with 12–6 or 8–4 Lennard–Jones potentials. They observed that in large volumes the bcc lattice always transformed through a martensitic transformation into one of the mechanically stable, fcc or hcp, structures. In small volumes (diameter < 100 nm) the same transformation took place only with the 12–6 potential, while the 8–4-type lattice did not exhibit a martensitic transformation and remained bcc. Stability of bcc structure in confining geometries, which remained unexplained in Ref. [49], may be understood if we assume that bcc phase is ANP. Indeed, mechanical instability of the bcc lattice occurs because the elastic stiffness of this structure is negative for both types of potentials [50]. As strain is the transition parameter for martensitic transformations, $f_{\eta\eta}$ plays the role of the elastic stiffness and the bcc structure may be interpreted as the transition state γ between two stable configurations, α and β (fcc and hcp). Mechanical calculations of [50] show that the absolute value of the 12–6-type lattice elastic stiffness is approximately seven times greater than that of the 8–4 lattice, that is $U_{12\text{-}6} \approx 7U_{8\text{-}4}$ because $U \sim |f_{\eta\eta}|$, see Eqs. (15b) and (16). Therefore, we find that the first condition of ANP stability, $U < U_{cr}$, may be satisfied for 8–4-type lattice and not satisfied for 12–6 one because the isothermal stiffness of the latter is "too negative".

Another example of ANP may be found in the study by Kim, Lin and Kelly [51] of solidification of submicron droplets, 10–60 nm, of high purity elemental metals by electrohydrodynamic atomization in vacuum when droplets solidify in the free flight. They found that under extreme conditions of high cooling rates and very small liquid volumes some pure metals solidified from the melt as an amorphous phase and that the critical size increased with decreasing melting temperature of each bcc metal except iron. The combination of high cooling rates and small volumes of particles as the necessary conditions for amorphization allows us to interpret the amorphous phase as ANP. Then the magnitudes of the thermodynamic number U for pure metals, Eq. (13) and Table 1, explain why some of them do exhibit amorphous states and some don't.

Acknowledgments

References

[1] J.S. Langer, Rev. Modern Phys. 52 (1980) 1;
P. Pelce (Ed.), Dynamics of Curved Fronts, Academic Press, London, 1988;
H. Yoshioka, Y. Tada, K. Kunimine, T. Furuichi, Y. Hayashi, Acta Mater. 54 (2006) 757.

[2] A. Karma, W.-J. Rappel, Phys. Rev. E 53 (1996) R3017;
A. Karma, W.-J. Rappel, Phys. Rev. E 57 (1998) 4323;
R.F. Almgren, SIAM J. Appl. Math. 59 (1999) 2086.

[3] L.D. Landau, Phys. Zs. Sowjet. 11 (26) (1937) 545;
See also D. Ter Haar (Ed.), Collected Papers of L.D. Landau, Gordon and Breach, London, 1967, p. 193, 209.

[4] J.D. van der Waals, Z. Phys. Chem. 13 (1894) 716.

[5] L.D. Landau, Phys. Zs. Sowjet. 12 (1937) 123;
See also D. Ter Haar (Ed.), Collected Papers of L.D. Landau, Gordon and Breach, London, 1967, p. 236.

[6] V.L. Ginzburg, L.D. Landau, Zh. Eksp. Teor. Fiz. 20 (1950) 1064.

[7] A. Novick-Cohen, Physica D 27 (1987) 260;
A.A. Wheeler, W.J. Boettinger, G.B. McFadden, Phys. Rev. A 45 (1992) 7424;
Y. Wang, A.G. Khachaturyan, Acta Mater. 45 (1997) 759;
G. Rubin, A.G. Khachaturyan, Acta Mater. 47 (1999) 1995.

[8] J.W. Cahn, J.E. Hilliard, J. Chem. Phys. 28 (1958) 258.

[9] J.W. Gibbs, The Scientific Papers, vol. 1, Dover, New York, 1961, p. 229.

[10] L.D. Landau, E.M. Lifshitz, Statistical Physics, 3rd ed., Pergamon Press, Oxford, 1980.

[11] A. Umantsev, Phys. Rev. B 64 (2001) 075419.

[12] A. Umantsev, J. Chem. Phys. 116 (2002) 4252.

[13] P. Winternitz, A.M. Grundland, J.A. Tuszynski, J. Phys. C: Solid State Phys. 21 (1988) 4931;
A.E. Filippov, Yu.E. Kuzovlev, T.K. Soboleva, Phys. Lett. A 165 (1992) 159.

[14] A.G. Khachaturyan, R.A. Suris, Sov. Phys. Crystallogr. 13 (1968) 63;
W.I. Khan, J. Phys. C: Solid State Phys. 19 (1986) 2969;
A.M. Grundland, E. Infeld, G. Rowlands, P. Winternitz, J. Phys.: Condens. Matter. 2 (1990) 7143.

[15] A.R. Umantsev, A.L. Roytburd, Sov. Phys. Solid State 30 (1988) 651.

[16] Reference [9], p. 105.

[17] J.W. Christian, The Theory of Phase Transformations in Metals and Alloys, Pergamon, 1965, p. 418.

[18] L. Granasy, F. Igloi, J. Chem. Phys. 107 (1997) 3634.

[19] J.D. Gunton, M. Droz, Introduction to the Theory of Metastable and Unstable States, Springer-Verlag, Berlin, 1983.

[20] J. Feder, K.C. Russell, J. Lothe, G.M. Pound, Adv. Phys. 15 (1966) 111.

[21] I.S. Yakub, Sov. Phys. Solid. State 21 (1979) 310;
F.P. Ludwig, J. Schmelzer, A. Milchev, Phase Trans. 48 (1994) 237.

[22] P.C. Fife, G.S. Gill, Physica D 35 (1989) 267;   Phys. Rev. A 43 (1991) 843.

[23] A. Umantsev, G.B. Olson, Phys. Rev. A 46 (1992) R6132;   Phys. Rev. E 48 (1993) 4229.

[24] H. Metiu, K. Kitahara, J. Ross, J. Chem. Phys. 65 (1976) 393;
S.-K. Chan, J. Chem. Phys. 67 (1977) 5755.

[25] S.M. Allen, J.W. Cahn, Acta Metall. 27 (1979) 1085.

[26] A. Umantsev, Acta Mater. 46 (1998) 4935.

[27] I.M. Lifshitz, Sov. Phys. JETP 15 (1962) 939.

[28] A. Umantsev, J. Chem. Phys. 96 (1992) 605.

[29] A.Z. Patashinsky, M.V. Chertkov, Fiz. Tverd. Tela (Leningrad) 32 (1990) 509;   Sov. Phys. Solid State 32 (1990) 295;
S.A. Schofield, D.W. Oxtoby, J. Chem. Phys. 94 (1991) 2176.

[30] S.-C. Ngan, L. Truskinovsky, Mech. Phys. Solid. 47 (1999) 141;
A. Vainchtein, Cont. Mech. Therm. 15 (2003) 1.

[31] D.J. Wolkind, in: W.R. Wilcox (Ed.), Preparation and Properties of Solid State Materials, vol. 4, Dekker, New York, 1979, p. 111.

[32] W.A. Tiller, The Science of Crystallization. Microscopic Interfacial Phenomena, Cambridge University Press, Cambridge, 1991, p. 68, 99.

[33] A. Umantsev, S.H. Davis, Phys. Rev. A 45 (1992) 7195.

[34] A. Umantsev, V. Vinogradov, V. Borisov, Sov. Phys. Crystallogr. 31 (1986) 596.

[35] P.K. Galenko, M.D. Krivilov, S.V. Buzilov, Phys. Rev. E 55 (1997) 611.

[36] S.-C. Huang, M.E. Glicksman, Acta Metall. 29 (1981) 717.

[37] A. Dougherty, J.P. Gollub, Phys. Rev. Lett. 63 (1989) 7195.

[38] F. Seitz, The Modern Theory of Solids, McGraw-Hill, NY, 1940, p. 480.

[39] A. Umantsev, J. Chem. Phys. 107 (1997) 1600.

[40] E.J. Gonzalez, et al., J. Mater. Res. 15 (2000) 764;
A. Salazar, et al., Anal. Sci. 17 (2001) s95;
R.L. Voti, et al., J. Optoel. Adv. Mater. 3 (2001) 779.

[41] T. Suzuki, S. Toyoda, T. Umeda, Y. Kimura, J. Crystal Growth 38 (1977) 123–128.

[42] R. Willnecker, D.M. Herlach, B. Feuerbacher, Phys. Rev. Lett. 62 (1989) 2707.

[43] M.E. Glicksman, R.J. Schaefer, J. Crystal Growth 1 (1967) 297–310;
L.A. Tarshis, G.R. Kotler, J. Crystal Growth 2 (1968) 222–226.

[44] M.E. Glicksman, R.J. Schaefer, J.D. Ayers, Metall. Trans. A 7A (1976) 1747.

[45] J.P. Franck, J. Jung, J. Low Temp. Phys. 64 (1986) 165.

[46] G.H. Rodway, J.D. Hunt, J. Cryst. Growth 112 (1991) 554.

[47] M.I. Mendelev, J. Schmalain, C.Z. Wang, J.R. Morris, K.M. Ho, Phys. Rev. B 74 (2006) 104206.

[48] S. Kajiwara, S. Ohno, K. Honma, Phil. Mag. A 63 (1991) 625–644.

[49] T. Suzuki, K. Takahashi, Mater. Trans. JIM 33 (1992) 184.

[50] M. Born, K. Huang, Dynamical Theory of Crystal Lattices, Clarendon Press, Oxford, 1954;
L.D. Landau, E.M. Lifshitz, Theory of Elasticity, Pergamon Press, Oxford, 1958.

[51] Y.-W. Kim, H.-M. Lin, T.F. Kelly, Acta Metall. 37 (1989) 247.

[52] O. Penrose, P. Fife, Physica D 43 (1990) 44;
S.-L. Wang, et al., Physica D 68 (1993) 189.

[53] G. Caginalp, Arch. Ration. Mech. 92 (1986) 207;
J.B. Collins, H. Levine, Phys. Rev. B 31 (1985) 6119.

[54] L.I. Rubinstein, The Stefan Problem, AMS, Providence, RI, 1971, pp. 141–189.

[55] J. Rosenthal, Trans. ASME 68 (1946) 849.

[56] The case of $T_0 = T_E - L/C$ was considered in A. Umantsev, Sov. Phys. Crystallogr. 30 (1985) 87.

[57] J.J. Hoyt, M. Asta, A. Karma, Mater. Sci. Eng. R 41 (2003) 121.